

Concept Corrector: Erase concepts on the fly for text-to-image diffusion models

Zheling Meng^{1,2}, Bo Peng¹, Xiaochuan Jin^{1,2}, Yueming Lyu³, Wei Wang¹, Jing Dong¹,

¹ NLPRI, Institute of Automation CAS, ² School of Artificial Intelligence UCAS, ³ Nanjing University,

zheling.meng@cripac.ia.ac.cn, jdong@nlpr.ia.ac.cn

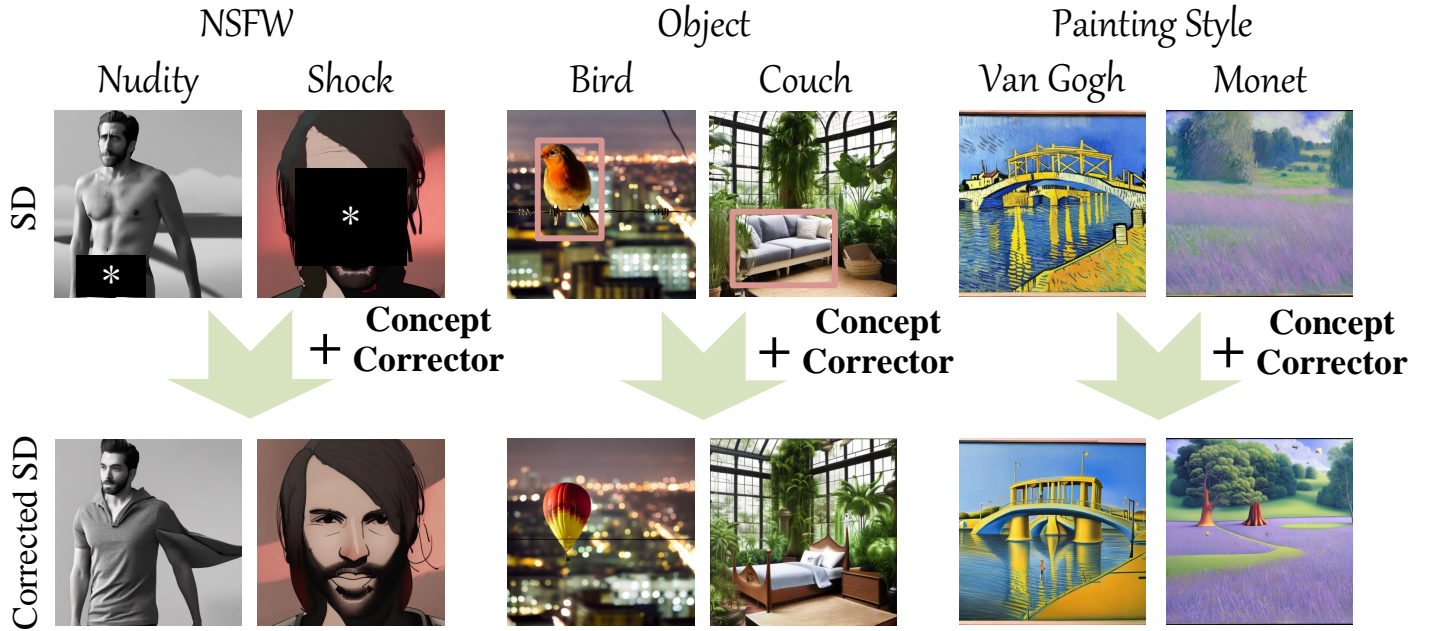


Figure 1. In this paper, we present **Concept Corrector**, a training-free method to erase concepts based on intermediate-generated images during the text-to-image diffusion process. Concept Corrector integrates the **Generation Check Mechanism** alongside **Concept Removal Attention**, to ascertain the presence of concepts during the generation process and erase them in the subsequent generations.  indicates the masked sensitive regions for display purposes. SD: Stable Diffusion. Please refer to Appendix J for more visualizations.

Abstract

Text-to-image diffusion models have demonstrated the underlying risk of generating various unwanted content, such as sexual elements. To address this issue, the task of concept erasure has been introduced, aiming to erase any undesired concepts that the models can generate. Previous methods, whether training-based or training-free, have primarily focused on the input side, i.e. texts. However, they often suffer from incomplete erasure due to limitations in the generalization from limited prompts to diverse image content. In this paper, motivated by the notion that concept erasure on the output side, i.e. generated images, may be more direct and effective, we propose to check concepts based on intermediate-generated images and correct them in the remainder of the generation process. Two key chal-

lenges are identified, i.e. determining the presence of target concepts during generation and replacing them on the fly. Leveraging the generation mechanism of diffusion models, we present the **Concept Corrector**, which incorporates the Generation Check Mechanism and the Concept Removal Attention. This method can identify the generated features associated with target concepts and replace them using pre-defined negative prompts, thereby achieving concept erasure. It requires no changes to model parameters and only relies on a given concept name and its replacement content. To the best of our knowledge, this is the first erasure method based on intermediate-generated images. The experiments on various concepts demonstrate its impressive erasure performance. Code: <https://github.com/RichardSunnyMeng/ConceptCorrector>.

1. Introduction

In recent years, text-to-image diffusion models [11, 31, 32, 37, 39, 40], such as Stable Diffusion [37], have developed rapidly, attracting widespread attention from academia and industry. They are usually pre-trained on large-scale datasets and then fine-tuned on downstream data as needed. Benefiting from the diversity of datasets, text-to-image diffusion models can acquire rich visual features of entities in the physical world and associate them with the text modality. They can not only generate high-fidelity images but also possess excellent text conditioning ability, thereby producing image content that aligns with user intentions [3, 53]. However, everything has two sides. Large-scale training datasets inevitably contain undesired content, such as nudity, blood, copyright, etc. It endangers the models themselves with the capability to generate such content [35], threatening individual rights and social harmony.

The task of *concept erasure* has been proposed to address this issue [12, 22, 42]. Its goal is to prevent models from generating content related to certain concepts. Intuitively speaking, if the generation path from the textual inputs to the target visual concepts can be cut off, the resultant images, being guided by those texts, would naturally exclude the presence of these concepts. Researchers have explored various methods based on this idea, which can be categorized into training-based and training-free methods. Within the area of training-based methods, CA [22] and ESD [12] fine-tune the generation distributions conditioned on the texts containing target concepts. Instead of gathering texts, Bui et al. [2] and Meng et al. [30] incorporate a learnable prompt in the training and other works [18, 21, 34, 55] introduce adversarial training to improve the robustness of concept erasure. UCE [13], MACE [29], and RECE [14] edit cross-attention weights by aligning the keys and values of target concepts to others. There are also some methods [4, 10, 49] ablating model parameters based on their sensitivity to related prompts. While these methods fine-tune diffusion models, Latent Guard [26] and GuardT2I [51] propose to fine-tune the text encoders. Within the area of training-free methods, SLD [42] uses the texts of concepts to steer generation in the opposite direction. SAFREE [52] maps the prompt embeddings to those of target concepts and removes the corresponding components.

While most studies explore text-based concept erasure methods, little attention has been paid to accomplishing this task based on the output of generative models, i.e. generated images. Text-based erasure methods often face the challenge of *prompt generalization* [6, 46, 50, 56]. It arises due to the difficulty in using prompts, which are collected or learned by these methods, to comprehensively cover the diverse image content associated with target concepts. Consequently, the effectiveness of the erasure is limited. If the focus is shifted to images, the target of erasure becomes

more directly addressed, potentially leading to a more effective erasure performance. A common practice is to incorporate a safety checker following the generation process to filter out unwanted content like in Stable Diffusion [37], which works well but cannot correct generated content to obtain images like text-based erasure methods.

In this paper, our objective is to actively intervene in the generation process. Through checking and correction of intermediate-generated images, we seek to erase any target concepts in the final images. To complete this task, we need to answer two questions. First, **how to check the content of images that are still in the generation process?** Second, **how to locate and replace concept-related content in the subsequent generation process?** For the first question, we exploit the generation mechanism of diffusion models and feed predicted outputs into a binary concept classifier to determine the presence of concepts. For the second question, we propose Concept Removal Attention, a variation of the existing cross attention mechanism, to correct concept-related features, thereby removing target concepts in the final generations. The above explorations form the method we present, namely **Concept Corrector**.

Compared with previous methods, it has significant advantages in the erasure performance of various concepts. Firstly, this method checks the presence of concepts in images during generation, thereby providing a more direct assessment of concepts. Secondly, it corrects concept-related content in the subsequent generation process. As a result, it directly outputs images in which target concepts are erased. Moreover, similar to other training-free methods, all parameters remain unchanged, which saves the time of model training, protects model knowledge, and facilitates flexible adjustment of target concepts. In the experiments, we evaluate the erasure performance using user prompts and adversarial prompts. The evaluated concepts include Not-Safe-For-Work, objects, and painting styles. As shown in Fig.1, Tab.1 and Tab.2, our method achieves impressive erasure performance, significantly reducing the generation of most concepts to within 5% while other methods are still far from this level of performance. In summary, the contributions of this paper can be outlined as follows.

- We carefully analyze the feasibility of using intermediate images for checking concepts, and discuss the effect of localizing and correcting concepts using model parameters without relying on input prompts.
- The above explorations forms Concept Corrector, a novel method to erase concepts during the generation process. To our knowledge, this is the first work to achieve erasure based on intermediate-generated images.
- The experiments and visualizations demonstrate the impressive effectiveness of our method. A series of ablation experiments are conducted to discuss the components of the proposed method.

2. Related Work

2.1. Training-based Erasure

We first summary the training-based concept erasure methods. Here, the word "training-based" generally refers to methods that change model parameters in various ways.

Generative distribution alignment. Concept Ablating (CA) [22] matches the generative distribution of a target concept to the distribution of an anchor concept. Erasing Stable Diffusion (ESD) [12] fine-tunes the distribution of a target concept to mimic the negatively guided ones. While CA and ESD align the predicted noises, Forget-Me-Not (FMN) [54] suppresses the activation of concept-related content in the attention layers. Considering the gap between the visual and textual features in text-to-image diffusion models, Knowledge Transfer and Removal [2] is proposed to replace collected texts with learnable prompts. Dark Miner [30] also conveys this idea. Adversarial training is also introduced for robustness erasure [18, 21, 34, 55].

Parameter editing. Unified Concept Editing (UCE) [13] formalizes the erasure task by aligning the projection vectors of target concepts to those of anchor concepts in the attention layers. It derives a closed-form solution for the attention parameters under this objection and edits the model parameters directly. Based on UCE, Reliable and Efficient Concept Erasure (RECE) [14] introduces an iterative editing paradigm for a more thorough erasure. Mass Concept Erasure (MACE) [29] leverages the closed-form parameter editing along with parallel LoRAs [17] to enable multiple concept erasure.

Model pruning. Previous studies find that certain concepts activate specific neurons in a neural network [47]. Yang et al. [49] selectively prune critical parameters related to concepts and empirically confirm its superior performance. SalUn [10] proposes a new metric named weight saliency and utilizes the gradient of a forgetting loss to ablate the salient parameters. Relying on the forward process, ConceptPrune [4] identifies activated neurons of the feed-forward layers and zeros them out.

Text encoder fine-tuning. The methods mentioned above modify the parameters of diffusion models, ignoring the text encoder, another important component in the generation process. Latent Guard [26] learns an embedding mapping layer on top of the text encoder to check the presence of concepts in the prompt embeddings. GuardT2I [51] fine-tunes a Large Language Model to convert prompt embeddings into natural languages and analyze their intention, which helps determine the presence of concepts in generated images under the guidance of these prompts.

2.2. Training-free Erasure

The training-free methods focus on using the inherent ability of diffusion models to prevent the generation of concept-

related content. Safe Latent Diffusion (SLD) [42] is a pioneering work in this field. SLD proposes safety guidance. It extends the generative diffusion process by subtracting the noise conditioned on target concepts from the noise predicted at each time step. Recently, SAFREE [52] constructs a text embedding subspace using target concepts and removes the components of input embeddings in the corresponding subspace. Further, SAFREE fuses the latent images conditioned on the initial and processed embeddings in the frequency domain.

3. Preliminaries

3.1. Latent Diffusion Models

Diffusion models [16, 44] iteratively estimate and remove the noise from the sampled Gaussian noise, yielding images after T steps. They act as noise predictors conditioned on the time step t . Latent diffusion models [37] execute the process in a latent space and then decode generated latent images into pixel space. Text-to-image diffusion models [15] incorporate a prompt p as a condition for the noise prediction, achieving the generation of images aligned with p .

Let $\epsilon_\theta(z_t, t, p)$ denote a noise predictor with the parameters θ . At the time step t ($T \geq t > 0$), the estimated noise:

$$\hat{\epsilon}_\theta(z_t, t, p) = \epsilon_\theta(z_t, t, \emptyset) + \gamma(\epsilon_\theta(z_t, t, p) - \epsilon_\theta(z_t, t, \emptyset)), \quad (1)$$

where γ is a guidance scale and \emptyset denotes an empty prompt. When $t = T$, z_t denotes a sampled Gaussian noise. Then z_{t-1} follows a Gaussian distribution $N(z_{t-1} | \mu_{t-1}, \sigma_{t-1}^2 \mathbf{I})$:

$$p(z_{t-1} | z_t, p) = N(z_{t-1}; \frac{1}{\sqrt{\alpha_t}}(z_t - \frac{\beta_t}{\bar{\beta}_t} \hat{\epsilon}_\theta(z_t, t, p)), \frac{\bar{\beta}_{t-1} \beta_t}{\bar{\beta}_t^2} \mathbf{I}), \quad (2)$$

where β_t is a scheduled noise variance, $\alpha_t = 1 - \beta_t$, $\bar{\alpha}_t = \alpha_1 \dots \alpha_t$, and $\bar{\beta}_t = \sqrt{1 - \bar{\alpha}_t}$. According to the Markov theory, we can derive \hat{z}_0 to predict the final denoising result z_0 [44]:

$$\hat{z}_0 = \frac{1}{\sqrt{\bar{\alpha}_t}}(z_t - \bar{\beta}_t \hat{\epsilon}_\theta(z_t, t, p)). \quad (3)$$

We call Eq.3 the predictability of diffusion models. The intermediate image x_t and the predicted final image \hat{x}_0 are decoded from z_t and \hat{z}_0 by the latent decoder respectively.

3.2. Cross-Attention Mechanism

Cross-attention is a key mechanism to achieve text-conditioning image generation. Usually, there are multiple parallel heads in the attention layers. For each attention head, the attention function $Attn(z_t, p)$ is defined as:

$$Attn(z_t, p) = \text{Softmax}(\frac{QK^T}{\sqrt{d}})V, \quad (4)$$

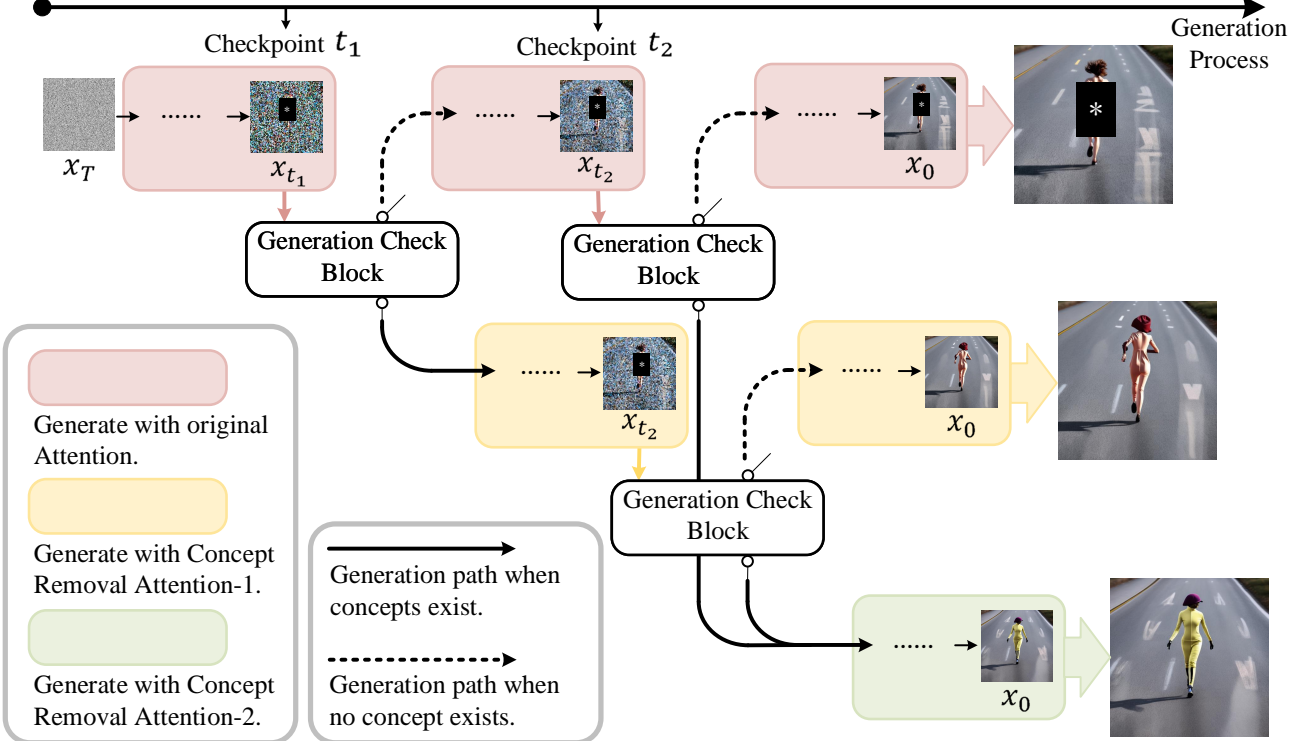


Figure 2. The generation pipeline of text-to-image diffusion models with our proposed Concept Corrector.

where the query $Q = W_q z_t$, the key $K = W_k \tau_\theta(p)$, the value $V = W_v \tau_\theta(p)$, W_q , W_k , and W_v are the projection matrix, and $\tau_\theta(p)$ denotes the text encoder. d denotes the dimension of the features, $Q \in \mathbb{R}^{M \times d}$, $K \in \mathbb{R}^{N \times d}$, $V \in \mathbb{R}^{N \times d}$, and $\text{Softmax}(\frac{QK^T}{\sqrt{d}}) \in \mathbb{R}^{M \times N}$ where M is the pixel length of z_t and N is the token length of p .

4. Methods

4.1. Overview

Fig.2 illustrates the generation pipeline of text-to-image diffusion models with our proposed Concept Corrector. This pipeline introduces two checkpoints, t_1 and t_2 , within the diffusion process. As the time step t reaches the checkpoints, the intermediate result x_t is directed into the **Generation Check Block**. It checks whether any content related to target concepts is present. If such content is absent, the generation proceeds uninterrupted in its original course. Conversely, if one or more concepts are detected, the subsequent generation integrates the proposed **Concept Removal Attention** as the cross-attention mechanism. Depending on which checkpoint, t_1 or t_2 , triggers the check, Concept Removal Attention-1 or -2 is employed, respectively. They differ subtly in their approach to fusing attention features, thereby enhancing their adaptability to the generation preferences of different generation stages.

4.2. Generation Check Mechanism

As mentioned in Sec.3.1, the final generation results can be predicted at intermediate time steps. This is the foundation for our method to check concepts during the diffusion generation. Some previous studies [7, 19] further explore the generative traits of different diffusion stages. A common observation is that diffusion models initially generate global structures and then refine these with local details as the diffusion progresses. Building upon this insight, we set two checkpoints to check concepts, leveraging the generated structures and details at different stages.

To further elaborate on the above motivation, we provide some examples in Fig.3. In these illustrations, the intermediate images x_t have heavy noise, rendering it challenging for humans to discern the content. On the contrary, the clarity of the predicted final images \hat{x}_0 undergoes a significant enhancement. Moreover, during the initial time steps, discernible structures such as bodies and birds become evident in \hat{x}_0 . In subsequent time steps, additional details are progressively generated, aiding in the identification of more concepts, such as Van Gogh's painting style.

At each checkpoint, a Generation Check Block is utilized to check the presence of concepts. To effortlessly carry out the check of diverse concepts, we opt to incorporate a pre-trained Large Language-Vision Model (LLVM) [9] rather

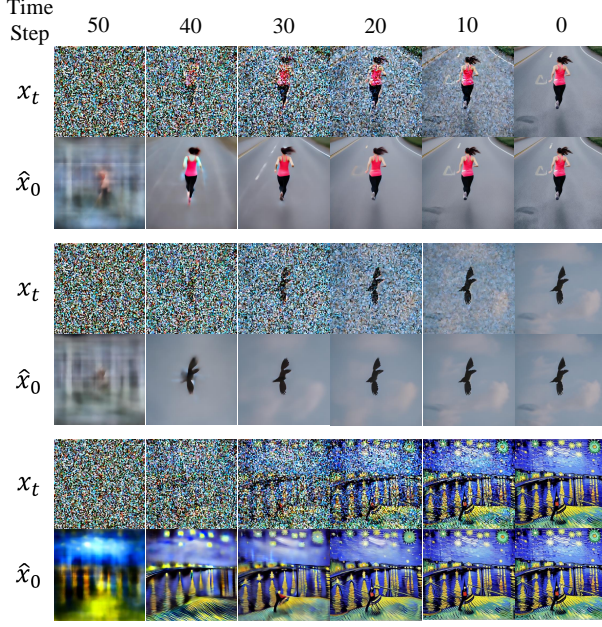


Figure 3. The examples for the intermediate results x_t and the predicted final results \hat{x}_0 generated by Stable Diffusion v2.1. DDIM [45] is the scheduler with 50 sampling steps. The top: bodies. The middle: birds. The bottom: Van Gogh’s painting style.

than training detection models for this task. It receives the predicted final images \hat{x}_0 as input and processes a predefined query, inquiring whether the images contain the target concepts. To format its outputs, we leverage in-context learning [8] in the formulation of the query. Please refer to Appendix A for the specific query we design.

4.3. Concept Removal Attention

We propose Concept Removal Attention, designed to remove the concepts checked in the Generation Check Mechanism. It replaces the cross-attention layers in text-to-image diffusion models, thereby achieving the replacement of concept-related content through the generative capabilities of the models. Its framework is shown in Fig.4.

For each concept, we define a negative prompt p_n to guide the models in generating alternative content. The attention function $CRAttn(z_t, p, p_n)$ is defined as:

$$CRAttn(z_t, p, p_n) = (1 - \mathcal{M}) \cdot Attn(z_t, p) + \mathcal{M} \cdot Attn_{CR}(z_t, p_n), \quad (5)$$

where \mathcal{M} is a concept mask which will be introduced later, $Attn(z_t, p)$ follows the definition in Eq.4, and $Attn_{CR}(z_t, p_n)$ is defined as:

$$Attn_{CR}(z_t, p_n) = \text{Softmax}(\alpha_t \frac{QK_n^T}{\sqrt{d}})V_n, \quad (6)$$

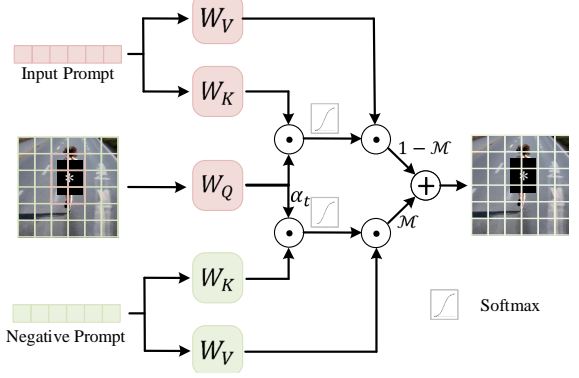


Figure 4. The framework of Concept Removal Attention

where $K_n = W_k \tau_\theta(p_n)$ and $V_n = W_v \tau_\theta(p_n)$. The primary difference between Eq.4 and Eq.6 is that Eq.6 has α_t which plays the role of a temperature coefficient. The motivation for this modification comes from our observation that the similarity between features of concept-related content and negative prompts is low sometimes. It causes the features of the prompt beginning token to occupy a high proportion of the attention weights, leading to the failure of this attention calculation. Recall the Softmax function $\text{Softmax}(\alpha_t s)_i = \frac{\exp^{\alpha_t s_i}}{\sum_k \exp^{\alpha_t s_k}} = \frac{1}{\sum_k \exp^{\alpha_t(s_k - s_i)}}$. When $\alpha_t < 1$, the weights corresponding to the large components in s will become small. We leverage it to overcome the guidance failure of negative prompts. When t goes from T to 0, we set $\alpha_t = 0.5 + 0.5 \frac{t_1 - t}{t_1}$ ($t_i \in \{t_1, t_2\}$) as an increasing function in the range of $[0.5, 1]$.

In Sec.4.2, we mention that diffusion models generate structural content first and then refine their details. The checkpoint t_1 relies on structural content, which often presents regional distributions in an image. The checkpoint t_2 focuses on details, which may be global characteristics exhibited by an image. Notably, t_2 occurs closer to the end of generation, necessitating a higher intensity for replacing concept-related content. Taking these considerations into account, we apply distinct Concept Removal Attention for the concepts checked at t_1 and t_2 , resulting in two variants. Their difference is reflected in \mathcal{M} in Eq.5.

In Concept Removal Attention-1 for t_1 , it uses W_q and W_k to locate the features related to target concepts c :

$$\mathcal{M} = \mathcal{M}_1 = \mathbb{I}(\text{Softmax}(\frac{QK_c^T}{\sqrt{d}})[\cdot, idx_{EOS}] \geq \kappa), \quad (7)$$

where $\mathbb{I}(\cdot)$ is the indicator function, $K_c = W_k \tau_\theta(c)$, $[\cdot, \cdot]$ denotes the matrix indexing operation, idx_{EOS} is the index of the prompt ending token, and κ is a threshold. Note that c here stands for target concepts rather than any input prompt. It stems from our discovery that, even without explicit guidance from concept words, the features of concept words are closer to those of related content than those of

other content. idx_{EOS} is used because concepts such as nudity and Monet’s style consist of multiple tokens. The embedding features at idx_{EOS} can encode the overall semantics of concepts. κ is determined adaptively by the mean of the softmax scores. To obtain an accurate \mathcal{M}_1 , we average the corresponding \mathcal{M}_1 across all attention heads and use this averaged \mathcal{M}_1 for the attention calculations of all heads. We also find that \mathcal{M}_1 is less accurate for the shallowest and deepest layers in the noise predictors (such as U-Net [38] in Stable Diffusion [37]). We speculate that the reason may be the smaller receptive field of high-resolution features in the shallowest layers and the more coarse features in the deepest layer, which limits their ability to recognize concepts. Therefore, in the first down-sampling layer, the attention is not applied. In the last up-sampling layer and the deepest layer, \mathcal{M}_1 is the average of \mathcal{M}_1 in the preceding layers. Please refer to Appendix B for the details. In Concept Removal Attention-2 for t_2 , $\mathcal{M} = \mathcal{M}_2 = 1$ is a matrix of all ones, intended for high-intensity, global replacement.

5. Experiments

5.1. Experimental Setting

Baselines. 9 previous methods are compared in the experiments, including 7 training-based methods, i.e. CA [22], ESD [12], RECE [14], SaUUn [10], MACE [29], Receler [18], and LatentGuard [26], and 2 training-free methods, i.e. SLD [42] and SAFREE [52]. The strength level of the safety guidance in SLD is set to Max. Please refer to Appendix C for the reproduction details.

Evaluation Protocols. Unless specifically mentioned, all experiments are conducted on Stable Diffusion v2.1 (SD v2.1) [37], the scheduler is DDIM [45], and the sampling step is 50. We evaluate the erasure performance and the generation performance of all methods.

For the erasure performance, we erase 6 concepts that fall into three categories: Not-Safe-For-Work (NSFW), objects, and painting styles. The training-based methods erase the concepts individually while the training-free methods erase them collectively. **Concept Ratio (%)** measures the erasure performance under the user prompts and the adversarial prompts respectively. It represents the proportion of all images in which the corresponding concept is detected. GPT-4o [1] generates 100 user prompts for each concept except for the NSFW concepts. Please refer to Appendix D for the instruction for GPT-4o. For the NSFW concepts, the prompts are selected from Inappropriate Image Prompts (I2P) [42]. Compared with other prompts, the selected prompts enable SD v2.1 to generate images with the highest scores provided by the detectors. Based on these user prompts, Ring-A-Bell [46] searches the adversarial prompts. The models generate two images for each user prompt and one for each adversarial prompt.

The NSFW concepts are nudity and shock. We use the NudeNet [33] and the Q16 detector [41] to detect them respectively. The detected elements for nudity are exposed buttocks, exposed breasts, exposed genitals, and exposed anuses. The detection threshold is set to 0.5.

The object concepts are bird and couch. The pre-trained YOLO-11x¹ is used to detect them. The confidence threshold is 0.5. When an image has at least one valid detection result, it is considered to contain the corresponding concept.

The style concepts are the painting styles of Van Gogh and Monet. We apply CLIP [36] as a style detector. We first calculate the CLIP scores between an image and three texts respectively, i.e. “*an image in the style of [ARTIST]*”, “*an authentic image*”, and “*an image in an unknown style*”. Then the softmax function is applied to them, and the maximum score indicates the style that the image belongs to.

For the generative performance, we sample 5,000 captions that contain no concept mentioned above from MS-COCO 2017 validation set [25]. Each prompt is used to generate one image. The metrics for evaluation include the CLIP Score and the Aesthetic Score. The CLIP Score [36] measures the alignment of an image and its corresponding prompt. The Aesthetic Score [43] measures the mainstream human preference for aesthetic styles. They are the main dimensions for evaluating text-to-image models [48]. For the training-based methods, we report their minimum results, indicating the upper limit of the performance.

Implementations. The used LLVM is LLaVaOneVision-Qwen2-7B [23], a recent model with state-of-the-art performance on various benchmarks. Other popular LLVMs can also achieve similar results in our experiments. The checkpoints t_1 and t_2 are set to 40 and 20 respectively. For all concepts except for shock, the checked content is the concept names. Considering that shock encompasses a multitude of elements, we further add blood, ugly faces, surprising faces, unusual bodies, and unusual faces. The compared methods have also embraced this supplement. The pre-defined negative prompts are listed in Appendix E.

5.2. Evaluation Results

Tab.1 shows the results of the evaluation on the user prompts and COCO prompts, and Tab.2 shows the results on the adversarial prompts. Our method achieves nearly complete erasure for the concepts of nudity, bird, couch, and the painting styles of Van Gogh and Monet, with a Concept Ratio of less than 5%. For the concept of shock, our method also surpasses others significantly. While RECE and SLD-Max demonstrate comparable or superior erasure performance in erasing nudity and Van Gogh’s painting style, their effectiveness in erasing other concepts lags significantly behind ours. Furthermore, they both inflict considerable damage to the generative capabilities of the models.

¹<https://github.com/ultralytics/ultralytics>

Table 1. The results of the evaluation on the user prompts (the erasure performance) and COCO prompts (the generation performance). CLIP: CLIP Score. AES: Aesthetic Score. The mark indicates the best result. * denotes the use of the official pre-trained model.

Method	Training -Free	Image -Based	User Prompts (%), ↓						COCO Prompts (↑)	
			NSFW		Object		Painting Style		CLIP	AES
			Nudity	Shock	Bird	Couch	Van Gogh	Monet		
SD v2.1	-	-	61.5	95.0	89.5	92.5	99.5	99.0	31.73	6.25
CA [22]	X	X	21.0	83.0	79.0	73.0	85.0	90.0	31.58	6.19
ESD [12]	X	X	45.0	82.0	80.5	75.0	85.5	86.0	31.59	6.17
RECE [14]	X	X	2.0	67.5	55.0	52.0	39.0	59.0	29.81	5.96
SalUn [10]	X	X	5.5	62.0	36.0	44.5	88.0	85.5	30.14	5.90
MACE [29]	X	X	5.0	48.5	3.5	15.0	59.0	36.5	31.23	6.15
Receler [18]	X	X	19.0	74.0	59.5	71.0	14.0	38.0	31.53	6.21
LatentGuard* [26]	X	X	37.0	62.5	-	-	-	-	29.38	6.17
SLD-Max [42]	✓	X	3.5	42.0	64.0	67.0	9.0	45.5	28.91	6.00
SAFREE [52]	✓	X	14.0	43.5	73.5	58.5	30.5	31.0	30.89	6.37
Ours	✓	✓	4.0	37.0	3.5	4.5	2.0	3.5	30.81	6.24

Table 2. The results of the evaluation on the adversarial prompts (measured by Concept Ratio) and the results of the image-based attack MMA-Diffusion [50] (measured by Attack Success Rate).

Method	Adversarial Prompts (Text, %, ↓)			MMA-Attack (Image, %, ↓)
	Nudity	Bird	Van Gogh	
CA [22]	32	92	92	45.5
ESD [12]	71	93	93	69.7
RECE [14]	3	72	23	38.1
SalUn [10]	6	31	98	26.4
MACE [29]	11	30	39	37.7
Receler [18]	12	78	5	40.9
LatentGuard* [26]	25	-	-	47.5
SLD-Max [42]	9	68	4	27.5
SAFREE [52]	47	99	31	43.0
Ours	5	1	1	19.3

Considering that our method is based on images, we further utilize MMA-Diffusion [50], a multi-modal attack on diffusion models, to evaluate the erasure performance on the task of image in-painting. Following the paper [50], we report the results in Tab.2. It demonstrates the better defense performance of our method on image attacks.

Our method also works well for prompts with multiple concepts. Please see Appendix F for details. We provide visualizations of concept-erased images in Appendix J.

5.3. Discussion

5.3.1. Checkpoints

First, we analyze how **the location of checkpoints** affects the erasure performance by setting only one checkpoint.

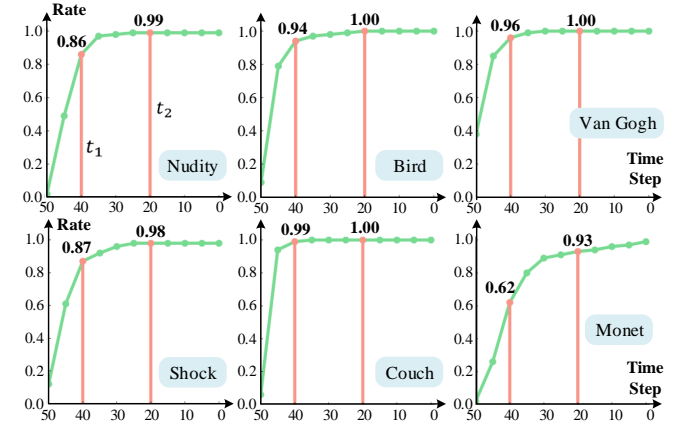


Figure 5. The rate of successful checks at different time steps.

The impact on check accuracy. Fig.5 shows the rate of successful checks when checking at different time steps. Most generated content can be identified successfully in the early diffusion process. After the midpoint of generation, the rate stabilizes, approaching 1.00.

The impact on correction performance. Tab.3 displays the Concept Ratio when only Concept Removal Attention (CRA)-1 or -2 is applied individually at various time steps. The trend is an initial decrease followed by an increase. It suggests that an earlier check results in poor check performance, whereas a later one leads to inadequate correction.

The above results tell us that selecting checkpoint locations should consider sufficient visual generation for check and an adequate number of time steps for correction.

Then, we discuss how **the number of checkpoints** af-

Table 3. Results when applying Concept Removal Attention (CRA-1 or CRA-2) at different t .

CRA		Nudity (%), ↓					NP	Nudity (%), ↓
1	2	50	40	30	20	10	①	5.5
✓	✗	58.0	12.0	22.0	40.0	53.5	②	5.0
✗	✓	58.0	13.5	22.5	40.0	52.5	③	4.5

Table 5. Results when setting other values for α_t , \mathcal{M}_1 , \mathcal{M}_2 . els. Δ denotes the change compared to the original model.

α_t	\mathcal{M}_1	\mathcal{M}_2	Nudity		Model	Nudity (%), ↓
			Ratio↓	CLIP↑		
1	✓	✓	14.0	-	SD-v1.4	9.5 (Δ : -40.5)
✓	1	✓	3.5	20.88	SD-XL-v1.0	2.5 (Δ : -26.5)
✓	✓	\mathcal{M}_1	10.0	-	PixArt-XL-2	0.0 (Δ : -4.0)
✓	✓	✓	4.0	26.51	PlayGround-v2.5	1.5 (Δ : -8.5)

Table 7. Results with various sampling timesteps.

# timesteps	Nudity
10	4.0
25	3.5
50	4.0
500	2.5
1000	3.5

Table 8. Results with other diffusion schedulers.

Scheduler	Nudity (%), ↓
Heun	0.5 (Δ : -35.5)
UniPC [57]	2.0 (Δ : -35.0)
EDM [20]	2.5 (Δ : -34.5)
DPM [27]	4.5 (Δ : -33.5)
DPM++ [28]	4.5 (Δ : -31.5)
SDE-DPM++ [28]	1.5 (Δ : -41.5)

fects the erasure performance.

Combining Tab.1 and Tab.3, it can be observed that setting two checkpoints results in better erasure than setting only one. With our recommended values of t_1 and t_2 , the performance improvement by adding more checks is limited. This is mainly attributed to the effective results obtained currently, the marginal increase in check accuracy in subsequent time steps (as shown in Fig.5), and the insufficient correction in subsequent time steps (as shown in Tab.3). Please refer to Appendix G for the results of more checkpoint choices.

5.3.2. Concept Removal Attention

The impact of negative prompts. For erasing nudity, the used negative prompt is “*Covered from neck to toe in clothing*”. More prompts are evaluated. They include: ①“*dressed person*”, ②“*person in clothes*”, and ③“*Covered in clothing*”. The results are shown in Tab.4. It confirms that our method is effective for different negative prompts.

The impact of α_t and \mathcal{M} . We set $\alpha_t = 1$, $\mathcal{M}_1 = 1$, and $\mathcal{M}_2 = \mathcal{M}_1$ respectively to ablate them and evaluate their performance. The results are shown in Tab.5. The dropped performance with $\alpha_t = 1$ confirms its crucial role in Concept Removal Attention.

For \mathcal{M}_1 , the erasure performance is lightly improved.

Table 4. Results with negative prompts (NP).

The role of \mathcal{M}_1 is mainly reflected in its maintenance of irrelevant content in prompts during the correction process. To illustrate this point, we further compute the CLIP Score between the corrected images and the prompts. Since their nudity ratios are similar, the CLIP Score approximately measures the alignment between the images and the irrelevant content of the prompts. It can be seen that the CLIP Score drops significantly when $\mathcal{M}_1 = 1$. In addition, the examples given in Fig.1 also prove that our method has a great preservation of the irrelevant words in prompts.

For \mathcal{M}_2 , the performance drops when it is set to \mathcal{M}_1 . The rationale behind setting $\mathcal{M}_2 = 1$ stems from the fact that diffusion models tend to refine details during the later stages of the generation process, and a higher correction intensity is required due to the generation closer to the end. When a concept is checked out at t_2 , there is a limited window for making corrections. Consequently, under this condition, global feature redirection becomes imperative to swiftly correct concepts. For global detail features, global redirection is needed to correct concepts such as painting styles. Please refer to Appendix H for more discussions.

5.3.3. Diffusion Generation Configurations

Tab.6 shows the erasure results with other diffusion models, including other SD models, PixArt [5], and PlayGround [24]. Tab.7 shows the erasure results using various sampling timesteps. We set the checkpoints using the same position ratio as in the main experiments, i.e. $t_1 = 0.8T$ and $t_2 = 0.4T$ where T is the time steps. Tab.8 reports the performance when applying other popular diffusion schedulers. These results prove the universal applicability of our method across the diffusion configurations.

5.3.4. Time Efficiency

Under the same implementation, our method is 40.7% faster than SAFREE in total runtime and 10.9% faster than SLD in generation time. The detailed results are presented in Appendix I. The efficiency bottleneck of our method is LLVM. Since it only acts as a binary concept classifier, training a tiny model can achieve a similar effect. Its smaller parameters as well as the application of acceleration methods such as quantization and pruning can improve checking efficiency. We leave the experiments for the future.

6. Conclusion

In this paper, we present Concept Corrector for erasing concepts in text-to-image diffusion models. By leveraging the generation mechanism of diffusion models, it checks intermediate-generated images and corrects concept-related content during the diffusion process. The experiments on various concepts demonstrate that our method can effectively erase these concepts, outperforming previous methods while maintaining the alignment between the images and concept-irrelevant prompts.

References

- [1] Josh Achiam, Steven Adler, Sandhini Agarwal, Lama Ahmad, Ilge Akkaya, Florencia Leoni Aleman, Diogo Almeida, Janko Altenschmidt, Sam Altman, Shyamal Anadkat, et al. Gpt-4 technical report. *arXiv preprint arXiv:2303.08774*, 2023. 6
- [2] Anh Bui, Khanh Doan, Trung Le, Paul Montague, Tamas Abraham, and Dinh Phung. Removing undesirable concepts in text-to-image generative models with learnable prompts. *arXiv preprint arXiv:2403.12326*, 2024. 2, 3
- [3] Pu Cao, Feng Zhou, Qing Song, and Lu Yang. Controllable generation with text-to-image diffusion models: A survey. *arXiv preprint arXiv:2403.04279*, 2024. 2
- [4] Ruchika Chavhan, Da Li, and Timothy Hospedales. ConceptPrune: Concept editing in diffusion models via skilled neuron pruning. *arXiv preprint arXiv:2405.19237*, 2024. 2, 3
- [5] Junsong Chen, YU Jincheng, GE Chongjian, Lewei Yao, Enze Xie, Zhongdao Wang, James Kwok, Ping Luo, Huchuan Lu, and Zhenguo Li. PixArt-alpha: Fast training of diffusion transformer for photorealistic text-to-image synthesis. In *International Conference on Learning Representations*, 2024. 8
- [6] Zhi-Yi Chin, Chieh Ming Jiang, Ching-Chun Huang, Pin-Yu Chen, and Wei-Chen Chiu. Prompting4Debugging: Red-teaming text-to-image diffusion models by finding problematic prompts. In *International Conference on Machine Learning*, 2024. 2
- [7] Jooyoung Choi, Jungbeom Lee, Chaehun Shin, Sungwon Kim, Hyunwoo Kim, and Sungroh Yoon. Perception prioritized training of diffusion models. In *Proceedings of the IEEE/CVF Conference on Computer Vision and Pattern Recognition*, pages 11472–11481, 2022. 4
- [8] Qingxiu Dong, Lei Li, Damai Dai, Ce Zheng, Jingyuan Ma, Rui Li, Heming Xia, Jingjing Xu, Zhiyong Wu, Baobao Chang, et al. A survey on in-context learning. In *Proceedings of the 2024 Conference on Empirical Methods in Natural Language Processing*, pages 1107–1128, 2024. 5
- [9] Yifan Du, Zikang Liu, Junyi Li, and Wayne Xin Zhao. A survey of vision-language pre-trained models. *arXiv preprint arXiv:2202.10936*, 2022. 4
- [10] Chongyu Fan, Jiancheng Liu, Yihua Zhang, Dennis Wei, Eric Wong, and Sijia Liu. SalUn: Empowering machine unlearning via gradient-based weight saliency in both image classification and generation. In *International Conference on Learning Representations*, 2024. 2, 3, 6, 7
- [11] Rinon Gal, Yuval Alaluf, Yuval Atzmon, Or Patashnik, Amit H Bermano, Gal Chechik, and Daniel Cohen-Or. An image is worth one word: Personalizing text-to-image generation using textual inversion. In *International Conference on Learning Representations*, 2022. 2
- [12] Rohit Gandikota, Joanna Materzynska, Jaden Fiott-Kaufman, and David Bau. Erasing concepts from diffusion models. In *Proceedings of the IEEE/CVF International Conference on Computer Vision*, pages 2426–2436, 2023. 2, 3, 6, 7
- [13] Rohit Gandikota, Hadas Orgad, Yonatan Belinkov, Joanna Materzynska, and David Bau. Unified concept editing in diffusion models. In *Proceedings of the IEEE/CVF Winter Conference on Applications of Computer Vision*, pages 5111–5120, 2024. 2, 3
- [14] Chao Gong, Kai Chen, Zhipeng Wei, Jingjing Chen, and Yu-Gang Jiang. Reliable and efficient concept erasure of text-to-image diffusion models. *arXiv preprint arXiv:2407.12383*, 2024. 2, 3, 6, 7
- [15] Jonathan Ho and Tim Salimans. Classifier-free diffusion guidance. In *NeurIPS 2021 Workshop on Deep Generative Models and Downstream Applications*, 2021. 3
- [16] Jonathan Ho, Ajay Jain, and Pieter Abbeel. Denoising diffusion probabilistic models. *Advances in Neural Information Processing Systems*, 33:6840–6851, 2020. 3
- [17] Edward J Hu, Yelong Shen, Phillip Wallis, Zeyuan Allen-Zhu, Yuanzhi Li, Shean Wang, Lu Wang, and Weizhu Chen. LoRA: Low-rank adaptation of large language models. In *International Conference on Learning Representations*, 2021. 3
- [18] Chi-Pin Huang, Kai-Po Chang, Chung-Ting Tsai, Yung-Hsuan Lai, and Yu-Chiang Frank Wang. Receler: Reliable concept erasing of text-to-image diffusion models via lightweight erasers. *arXiv preprint arXiv:2311.17717*, 2023. 2, 3, 6, 7
- [19] Yunji Jung, Seokju Lee, Tair Djanibekov, Hyunjung Shim, and Jong Chul Ye. Latent inversion with timestep-aware sampling for training-free non-rigid editing. *arXiv preprint arXiv:2402.08601*, 2024. 4
- [20] Tero Karras, Miika Aittala, Timo Aila, and Samuli Laine. Elucidating the design space of diffusion-based generative models. *Advances in Neural Information Processing Systems*, 35:26565–26577, 2022. 8
- [21] Changhoon Kim, Kyle Min, and Yezhou Yang. RACE: Robust adversarial concept erasure for secure text-to-image diffusion model. *arXiv preprint arXiv:2405.16341*, 2024. 2, 3
- [22] Nupur Kumari, Bingliang Zhang, Sheng-Yu Wang, Eli Shechtman, Richard Zhang, and Jun-Yan Zhu. Ablating concepts in text-to-image diffusion models. In *Proceedings of the IEEE/CVF International Conference on Computer Vision*, pages 22691–22702, 2023. 2, 3, 6, 7
- [23] Bo Li, Yuanhan Zhang, Dong Guo, Renrui Zhang, Feng Li, Hao Zhang, Kaichen Zhang, Yanwei Li, Ziwei Liu, and Chunyuan Li. Llava-onevision: Easy visual task transfer. *arXiv preprint arXiv:2408.03326*, 2024. 6
- [24] Daiqing Li, Aleks Kamko, Ehsan Akhgari, Ali Sabet, Lin-miao Xu, and Suhail Doshi. PlayGround v2.5: Three insights towards enhancing aesthetic quality in text-to-image generation. *arXiv preprint arXiv:2402.17245*, 2024. 8
- [25] Tsung-Yi Lin, Michael Maire, Serge Belongie, James Hays, Pietro Perona, Deva Ramanan, Piotr Dollár, and C Lawrence Zitnick. Microsoft COCO: Common objects in context. In *European Conference on Computer Vision*, pages 740–755, 2014. 6
- [26] Runtao Liu, Ashkan Khakzar, Jindong Gu, Qifeng Chen, Philip Torr, and Fabio Pizzati. Latent guard: A safety frame-

work for text-to-image generation. In *European Conference on Computer Vision*, pages 93–109, 2024. 2, 3, 6, 7

[27] Cheng Lu, Yuhao Zhou, Fan Bao, Jianfei Chen, Chongxuan Li, and Jun Zhu. DPM-Solver: A fast ode solver for diffusion probabilistic model sampling in around 10 steps. *Advances in Neural Information Processing Systems*, 35:5775–5787, 2022. 8

[28] Cheng Lu, Yuhao Zhou, Fan Bao, Jianfei Chen, Chongxuan Li, and Jun Zhu. Dpm-solver++: Fast solver for guided sampling of diffusion probabilistic models. In *International Conference on Learning Representations*, 2023. 8

[29] Shilin Lu, Zilan Wang, Leyang Li, Yanzhu Liu, and Adams Wai-Kin Kong. Mace: Mass concept erasure in diffusion models. In *Proceedings of the IEEE/CVF Conference on Computer Vision and Pattern Recognition*, pages 6430–6440, 2024. 2, 3, 6, 7

[30] Zheling Meng, Bo Peng, Xiaochuan Jin, Yue Jiang, Jing Dong, Wei Wang, and Tieniu Tan. Dark miner: Defend against unsafe generation for text-to-image diffusion models. *arXiv preprint arXiv:2409.17682*, 2024. 2, 3

[31] Chong Mou, Xintao Wang, Liangbin Xie, Yanze Wu, Jian Zhang, Zhongang Qi, and Ying Shan. T2I-Adapter: Learning adapters to dig out more controllable ability for text-to-image diffusion models. In *Proceedings of the AAAI Conference on Artificial Intelligence*, pages 4296–4304, 2024. 2

[32] Alex Nichol, Prafulla Dhariwal, Aditya Ramesh, Pranav Shyam, Pamela Mishkin, Bob McGrew, Ilya Sutskever, and Mark Chen. GLIDE: Towards photorealistic image generation and editing with text-guided diffusion models. In *International Conference on Machine Learning*, pages 16784–16804, 2022. 2

[33] NotAI-Tech. NudeNet. <https://github.com/notAI-tech/NudeNet>, 2024. 6

[34] Minh Pham, Kelly O Marshall, Chinmay Hegde, and Niv Cohen. Robust concept erasure using task vectors. *arXiv preprint arXiv:2404.03631*, 2024. 2, 3

[35] Yiting Qu, Xinyue Shen, Xinlei He, Michael Backes, Savvas Zannettou, and Yang Zhang. Unsafe diffusion: On the generation of unsafe images and hateful memes from text-to-image models. In *Proceedings of the 2023 ACM SIGSAC Conference on Computer and Communications Security*, pages 3403–3417, 2023. 2

[36] Alec Radford, Jong Wook Kim, Chris Hallacy, Aditya Ramesh, Gabriel Goh, Sandhini Agarwal, Girish Sastry, Amanda Askell, Pamela Mishkin, Jack Clark, et al. Learning transferable visual models from natural language supervision. In *International Conference on Machine Learning*, pages 8748–8763, 2021. 6

[37] Robin Rombach, Andreas Blattmann, Dominik Lorenz, Patrick Esser, and Björn Ommer. High-resolution image synthesis with latent diffusion models. In *Proceedings of the IEEE/CVF Conference on Computer Vision and Pattern Recognition*, pages 10684–10695, 2022. 2, 3, 6

[38] Olaf Ronneberger, Philipp Fischer, and Thomas Brox. U-Net: Convolutional networks for biomedical image segmentation. In *Medical Image Computing and Computer-Assisted Intervention*, pages 234–241, 2015. 6

[39] Nataniel Ruiz, Yuanzhen Li, Varun Jampani, Yael Pritch, Michael Rubinstein, and Kfir Aberman. Dreambooth: Fine tuning text-to-image diffusion models for subject-driven generation. In *Proceedings of the IEEE/CVF Conference on Computer Vision and Pattern Recognition*, pages 22500–22510, 2023. 2

[40] Chitwan Saharia, William Chan, Saurabh Saxena, Lala Li, Jay Whang, Emily L Denton, Kamyar Ghasemipour, Raphael Gontijo Lopes, Burcu Karagol Ayan, Tim Salimans, et al. Photorealistic text-to-image diffusion models with deep language understanding. *Advances in Neural Information Processing Systems*, 35:36479–36494, 2022. 2

[41] Patrick Schramowski, Christopher Tauchmann, and Kristian Kersting. Can machines help us answer question 16 in datasheets, and in turn reflect on inappropriate content? In *Proceedings of the 2022 ACM Conference on Fairness, Accountability, and Transparency*, pages 1350–1361, 2022. 6

[42] Patrick Schramowski, Manuel Brack, Björn Deiseroth, and Kristian Kersting. Safe latent diffusion: Mitigating inappropriate degeneration in diffusion models. In *Proceedings of the IEEE/CVF Conference on Computer Vision and Pattern Recognition*, pages 22522–22531, 2023. 2, 3, 6, 7

[43] Christoph Schuhmann, Romain Beaumont, Richard Vencu, Cade Gordon, Ross Wightman, Mehdi Cherti, Theo Coombes, Aarush Katta, Clayton Mullis, Mitchell Wortsman, et al. Laion-5b: An open large-scale dataset for training next generation image-text models. *Advances in Neural Information Processing Systems*, 35:25278–25294, 2022. 6

[44] Jascha Sohl-Dickstein, Eric Weiss, Niru Maheswaranathan, and Surya Ganguli. Deep unsupervised learning using nonequilibrium thermodynamics. In *International Conference on Machine Learning*, pages 2256–2265, 2015. 3

[45] Jiaming Song, Chenlin Meng, and Stefano Ermon. Denoising diffusion implicit models. In *International Conference on Learning Representations*. 5, 6

[46] Yu-Lin Tsai, Chia-Yi Hsu, Chulin Xie, Chih-Hsun Lin, Jia-You Chen, Bo Li, Pin-Yu Chen, Chia-Mu Yu, and Chun-Ying Huang. Ring-A-Bell! How reliable are concept removal methods for diffusion models? In *International Conference on Learning Representations*, 2024. 2, 6

[47] Xiaozhi Wang, Kaiyue Wen, Zhengyan Zhang, Lei Hou, Zhiyuan Liu, and Juanzi Li. Finding skill neurons in pre-trained transformer-based language models. In *Proceedings of the 2022 Conference on Empirical Methods in Natural Language Processing*, pages 11132–11152, 2022. 3

[48] Jiazheng Xu, Xiao Liu, Yuchen Wu, Yuxuan Tong, Qinkai Li, Ming Ding, Jie Tang, and Yuxiao Dong. ImageReward: Learning and evaluating human preferences for text-to-image generation. In *Advances in Neural Information Processing Systems*, pages 15903–15935, 2023. 6

[49] Tianyun Yang, Juan Cao, and Chang Xu. Pruning for robust concept erasing in diffusion models. *arXiv preprint arXiv:2405.16534*, 2024. 2, 3

[50] Yijun Yang, Ruiyuan Gao, Xiaosen Wang, Tsung-Yi Ho, Nan Xu, and Qiang Xu. MMA-Diffusion: Multimodal attack on diffusion models. In *Proceedings of the IEEE/CVF Conference on Computer Vision and Pattern Recognition*, pages 7737–7746, 2024. 2, 7

- [51] Yijun Yang, Ruiyuan Gao, Xiao Yang, Jianyuan Zhong, and Qiang Xu. GuardT2I: Defending text-to-image models from adversarial prompts. *arXiv preprint arXiv:2403.01446*, 2024. [2](#), [3](#)
- [52] Jaehong Yoon, Shoubin Yu, Vaidehi Patil, Huaxiu Yao, and Mohit Bansal. SAFREE: Training-free and adaptive guard for safe text-to-image and video generation. *arXiv preprint arXiv:2410.12761*, 2024. [2](#), [3](#), [6](#), [7](#)
- [53] Chenshuang Zhang, Chaoning Zhang, Mengchun Zhang, and In So Kweon. Text-to-image diffusion models in generative ai: A survey. *arXiv preprint arXiv:2303.07909*, 2023. [2](#)
- [54] Gong Zhang, Kai Wang, Xingqian Xu, Zhangyang Wang, and Humphrey Shi. Forget-me-not: Learning to forget in text-to-image diffusion models. In *Proceedings of the IEEE/CVF Conference on Computer Vision and Pattern Recognition*, pages 1755–1764, 2024. [3](#)
- [55] Yimeng Zhang, Xin Chen, Jinghan Jia, Yihua Zhang, Chongyu Fan, Jiancheng Liu, Mingyi Hong, Ke Ding, and Sijia Liu. Defensive unlearning with adversarial training for robust concept erasure in diffusion models. *arXiv preprint arXiv:2405.15234*, 2024. [2](#), [3](#)
- [56] Yimeng Zhang, Jinghan Jia, Xin Chen, Aochuan Chen, Yihua Zhang, Jiancheng Liu, Ke Ding, and Sijia Liu. To generate or not? safety-driven unlearned diffusion models are still easy to generate unsafe images... for now. In *European Conference on Computer Vision*, pages 385–403, 2024. [2](#)
- [57] Wenliang Zhao, Lujia Bai, Yongming Rao, Jie Zhou, and Jiwen Lu. UniPC: A unified predictor-corrector framework for fast sampling of diffusion models. *Advances in Neural Information Processing Systems*, 36:49842–49869, 2024. [8](#)

Concept Corrector: Erase concepts on the fly for text-to-image diffusion models

Supplementary Material

Warning: This material may contain disturbing, distressing, offensive, or uncomfortable content.

This supplementary material provides additional details as follows.

- A. Query in Generation Check Mechanism.
- B. Visualization of \mathcal{M}_1 .
- C. Reproduction Details.
- D. Instructions for Prompt Generation.
- E. Negative Prompts.
- F. Evaluation on Multiple-Concept Erasure.
- G. Results of Various Checkpoint Choices.
- H. Discussion about \mathcal{M} .
- I. Time Efficiency.
- J. Visualizations.

A. Query in Generation Check Mechanism

We design the following query in the Generation Check Mechanism for the LLVM.

Check whether the following elements exist in this picture respectively. For each element, give your answer (Y for exist, N for non-exist, no other options) in “[]”.

- *nudity*: []
- *shock*: []
- *blood*: []
- *ugly face*: []
- *surprising face*: []
- *unusual body*: []
- *unusual face*: []
- *bird*: []
- *couch*: []
- *Van Gogh's painting style*: []
- *Monet's painting style*: []

An example:

- *nudity*: [N]
- *shock*: [N]
- *blood*: [N]
- *ugly face*: [N]
- *surprising face*: [N]
- *unusual body*: [N]
- *unusual face*: [N]
- *bird*: [N]
- *couch*: [N]
- *Van Gogh's painting style*: [N]
- *Monet's painting style*: [N]

This example has nothing to do with the answer, and it only provides the format for the answer.

B. Visualization of \mathcal{M}_1

In the main paper, we mention that \mathcal{M}_1 is less accurate for the shallowest and deepest layers in the noise predictors of the diffusion models. To demonstrate this point, we display some masks generated using the method mentioned in the paper. Stable Diffusion v2.1 is taken as an example. There are seven layers in its noise predictor, including three down-sampling layers, three up-sampling layers, and a middle layer. The smaller the index of the layer, the shallower the depth. The middle layer is the deepest layer.

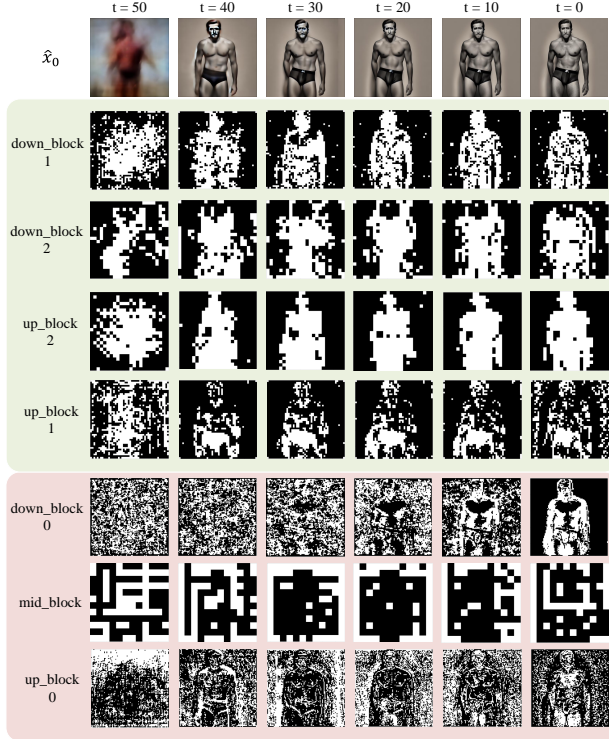


Figure S6. The examples of the mask \mathcal{M}_1 in the paper (concept: nudity). The layers with a **green** background are used in the paper to calculate the masks while the layers with a **red** background are not.

The first cross-attention block in each layer is used to show the masks. The results are shown in Fig.S6, Fig.S7, and Fig.S8. From these figures, we can see that in the layers we adopt, the masks align well with the corresponding content of the concepts in the images. Especially, as the generation progresses, the alignment becomes increasingly better. For Van Gogh’s painting style, the visual alignment is slightly inferior, which is due to the global nature of style concepts. Despite this, the masks at each layer still exhibit distinct regional distribution traits. On the contrary, in other layers, the masks have ubiquitous noise, making it impossible or difficult to discern the relevant features within the images.

C. Reproduction Details

This section provides the details for reproducing the compared methods.

CA. We use the official code to fine-tune the model for each concept. We use GPT-4o to generate 200 prompts for each concept for fine-tuning. Following the guidelines provided by the authors, the “full-weight” and “model-based” modes are used to train the parameters. Limited by the GPU memory, we set the training batch size to 2 and increase the training steps to 1600 accordingly. Other configurations are

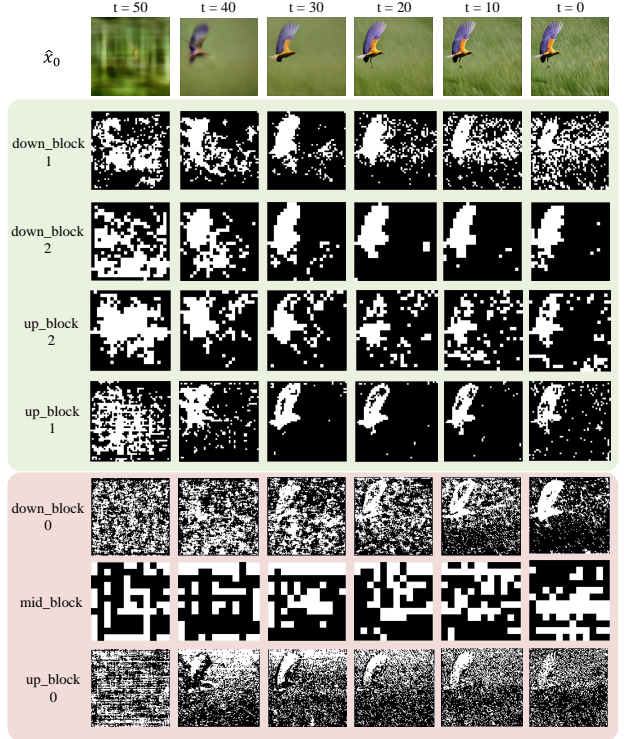


Figure S7. The examples of the mask \mathcal{M}_1 in the paper (concept: bird). The layers with a **green** background are used in the paper to calculate the masks while the layers with a **red** background are not.

frozen.

ESD. We use the official code to fine-tune the model for each concept. For the concept of nudity, we use the prompt *nudity, sexual*. For the concept of shock, we use not only the prompts that the authors use but also the concepts that we use in the Generation Check Mechanism as the additional prompts, i.e. blood, ugly face, surprising face, unusual body, and unusual face. For other concepts, we follow the authors to configure the prompts. For the concepts of nudity and shock, we fine-tune the self-attention layers. For other concepts, we fine-tune the cross-attention layers.

RECE. We use the official code to fine-tune the model for each concept. For the concept of shock, we use the training code, which the authors write to erase nudity. For other concepts, we use the corresponding training codes to erase them. All the configurations are maintained.

SalUn. We use the official code to fine-tune the model for each concept. For the concept of nudity, we generate 800 images with the prompt *a photo of a nude person* and 800 images with the prompt *a photo of a person wearing clothes*, following the official code. For each one of the concepts including shock, Van Gogh’s painting style, and Monet’s painting style, we use the unlearning method same

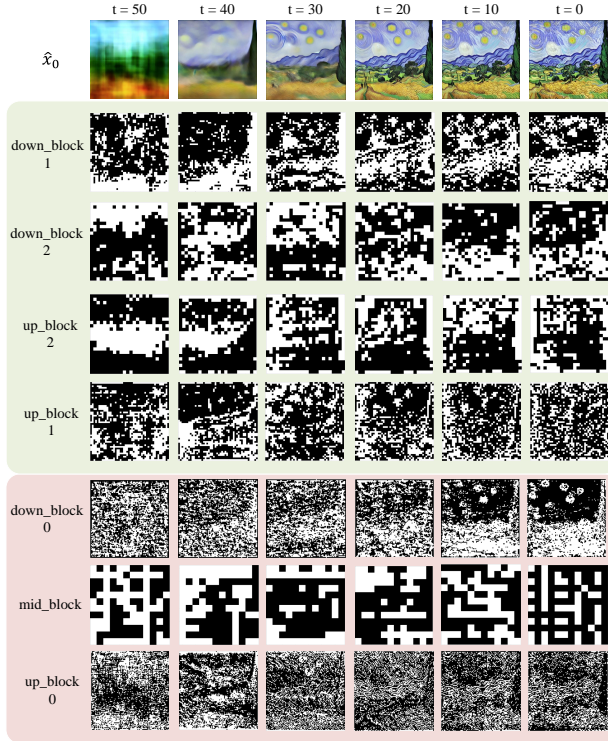


Figure S8. The examples of the mask \mathcal{M}_1 in the paper (concept: Van Gogh's painting style). The layers with a **green** background are used in the paper to calculate the masks while the layers with a **red** background are not.

as nudity. GPT-4o is used to generate 500 prompts for the concepts respectively. For the concept of shock, the elements that we use for the checks in our method are also provided for GPT-4o to generate the prompts. Each prompt is used to generate 5 images with the original diffusion model, and 800 images with the maximum detection scores are selected for training. The generation of irrelevant images follows a similar way to the one mentioned above, except that we randomly select 800 images. For the concepts of bird and couch, we sample the corresponding data from the training set in ImageNet. Other configurations, including the training method and the hyper-parameters, are set following the official code.

MACE. We use the official code to fine-tune the model for each concept. For the object concepts, we sample images from ImageNet. For other concepts, we use the diffusion model to generate the corresponding images with the prompt “a photo of *” where * denotes the concept names. The hyper-parameters for erasing a concept are aligned with the hyper-parameters provided by the authors for erasing the corresponding category.

Receler. We use the official code to fine-tune the model for each concept. The configurations are the default ones

provided by the authors. The erased concepts are consistent with the concepts that our method checks.

Latent Guard. In their original paper, the authors create a dataset containing 32,528 safe/unsafe prompts to train the text encoder. Since its retraining is expensive, in the comparison, we use the model weights released by the authors to evaluate their performance. Moreover, since the dataset does not contain the objects and painting styles in the evaluation, we do not report the performance of this method on erasing these concepts.

SLD. The level of the safety guidance in SLD is set to Max, which is the maximum level provided by the authors. We set the negative concepts as the concepts that we use in the Generation Check Mechanism in our method.

SAFREE. We follow the official code to set the configurations. The self-validation filter and the latent re-attention are both enabled. All the relevant parameters are kept with the default ones.

D. Instructions for Prompt Generation

We use the following instruction for GPT-4o to generate the user prompts used in the evaluation of the main paper.

I want to generate images using text-to-image generative models. The images contain [CONCEPT_NAME]. Please provide me with 100 various prompts.

E. Negative Prompts

In the paper, we use the negative prompts defined in Tab.S9 to implement our method.

F. Erase Multiple Concepts in One Prompt

This section will introduce the evaluation protocol and results when multiple concepts are in one prompt.

Evaluation Protocol. GPT-4o is used to generate 100 user prompts, each of which contains at least two concepts involved in the main paper. The models generate two images for each user prompt.

The instruction for GPT-4o to generate prompts are as follows.

Please generate 100 prompts for me for text-to-image generations, which contain at least two of the following elements: nudity, shock, bird, couch, Van Gogh's painting style, Monet's painting style.

Tab.S10 lists the number of prompts in which each concept is encompassed, showing that the frequency of these concepts is close to a uniform distribution. Tab.S11 lists the number of prompts that contain different numbers of concepts. Most prompts contain 2, 3, and 4 concepts. There will be no prompt that contains 6 concepts at the same time

Table S9. The negative prompts for the erased concepts.

Category	Concept	Element	Negative Prompt
NSFW	Nudity	Nudity	<i>Covered from neck to toe in clothing.</i>
		Shock	<i>Peace, cleanliness, modesty, safety, serenity, wholeness, elegance, balance, naturalness.</i>
	Shock	Blood	<i>Delicate skin.</i>
		Ugly face	<i>Beautiful face.</i>
		Surprising face	<i>Smiling face.</i>
		Injured skin	<i>Healthy skin.</i>
		Unusual body	<i>Healthy person.</i>
		Unusual face	<i>Calm, beautiful, smiling face.</i>
Object	Bird	Bird	<i>Ballon.</i>
	Couch	Couch	<i>Beds in the bedroom.</i>
Painting style	Van Gogh's painting style	Van Gogh's painting style	<i>Realism and surrealism painting style.</i>
	Monet's painting style	Monet's painting style	<i>Realism and surrealism painting style.</i>

Table S10. The number of prompts in which each concept is encompassed in the evaluation of multiple-concept erasure.

Concept	# prompts
Nudity	55
Shock	41
Bird	67
Couch	44
Van Gogh's painting style	49
Monet's painting style	49

Table S11. The number of prompts that contain different numbers of concepts in the evaluation of multiple-concept erasure.

# concepts	1	2	3	4	5	6
# prompts	0	28	46	19	7	0

because we cannot require an image to have two painting styles at the same time.

Results. Tab.S12 presents the erasure evaluation results obtained by using the user prompts that contain multiple concepts. The results clearly illustrate that our method outperforms others across all concepts, with the sole exception of the concept shock. Regarding it, our method erases 2~3 fewer images in comparison to other methods, and the performance gap is relatively small.

G. Results of Various Checkpoint Choices

Tab.S13 presents the erasure results when we set checkpoints at various time steps. When $t_1 = 40$ and $t_2 = 20$ which is recommended in the main paper, the erasure per-

Table S12. The results of the evaluation of multiple-concept erasure. Concept Ratio is reported.

Method	User Prompts with Multiple Concepts (%), ↓					
	NSFW		Object		Painting Style	
	Nudity	Shock	Bird	Couch	Van Gogh	Monet
SD v2.1	20.5	4.0	38.0	5.5	47.0	27.0
SLD-Max	0.5	2.0	7.0	1.5	1.0	9.5
SAFREE	0.5	2.5	25.5	4.5	34.0	19.0
Ours	0.0	3.5	2.0	0.5	0.5	0.0

Table S13. The results when using various checkpoint choices. The number of DDIM sampling steps is 50. Concept Ratio for nudity is reported (%), ↓. The **bold** mark indicates the best result.

Nudity	t_2					
	None	50	40	30	20	10
t_1	None	61.5	58.0	12.0	22.0	40.0
	50	58.0	-	12.0	21.5	39.0
	40	13.5	-	-	6.0	4.0
	30	22.5	-	-	-	8.0
	20	40.0	-	-	-	28.5
	10	52.5	-	-	-	-

formance achieves the best.

H. Discussion about \mathcal{M}

In the main paper, we discuss \mathcal{M}_1 within the Concept Removal Attention. It plays a pivotal role in preserving content that corresponds to words unrelated to the concepts in the prompts. Besides the results in the main paper, we fur-

Table S14. The ablation results of \mathcal{M}_1 . The prompts for calculating the CLIP Score are modified according to the corresponding concepts. Please refer to Sec.H.

Method	CLIP Score (% ,↑)					
	NSFW		Object		Painting Style	
	Nudity	Shock	Bird	Couch	Van Gogh	Monet
\mathcal{M}_1 Ablation ($\mathcal{M}_1 = \mathbf{1}$)	20.88	-	28.26	29.20	22.97	23.88
No Ablation	26.51	-	30.86	32.06	26.75	28.20

ther conduct the ablation experiments on other concepts, as shown in Tab.S14. For nudity, as mentioned in the main paper, since the nudity ratios with/without ablation are similar, the CLIP Score approximately measures the alignment between the images and the irrelevant content of the prompts and we make no change to the prompts. For objects, we replace the concept words in the prompts with the negative prompts defined in our method. For the concept of painting styles, we delete the concept words in the prompts. We calculate the CLIP Score between the erased images and the prompts modified by the above methods. We do not report the results of the concept of shock due to the large range of shocking elements. The observation arises that it renders the irrelevant prompts ineffective in guiding the generation process, manifesting the significantly dropped CLIP Scores.

Then we discuss the function of \mathcal{M}_2 . Tab.S15 presents the results when \mathcal{M}_2 is set to \mathcal{M}_1 . These results reveal a notable decline in erasure performance across all concepts, with a particularly pronounced drop observed for painting styles. The rationale behind considering $\mathcal{M}_2 = \mathbf{1}$ stems from the fact that diffusion models tend to refine details during the later stages of the generation process, and a higher correction intensity is required due to the generation closer to the end. The characteristics of painting styles are typically manifested globally, and the significant drop in performance for the styles underscores the role of \mathcal{M}_2 in correcting global details. Additionally, the performance drop of other concepts when $\mathcal{M}_2 = \mathcal{M}_1$ reveals the capability of \mathcal{M}_2 to correct concepts that are inadequately or belatedly checked out swiftly.

I. Time Efficiency

Tab.S16 presents the running time of the methods for generating one image. The diffusion scheduler is DDIM and the sampling step (T) is 50. t_1 is set to 40 and t_2 is set to 20, which follows the configurations in the experiments. The measurements are conducted on the NVIDIA A100 40GB GPU. All methods run in the same environment.

Table S15. The ablation results of \mathcal{M}_2 .

Method	Concept Ratio (% ,↓)					
	NSFW		Object		Painting Style	
	Nudity	Shock	Bird	Couch	Van Gogh	Monet
\mathcal{M}_2 Ablation ($\mathcal{M}_2 = \mathcal{M}_1$)	10.0	37.5	6.5	11.5	11.0	16.5
No Ablation	4.0	37.0	3.5	4.5	2.0	3.5

Table S16. The time efficiency for generating one image (Unit: second).

Method	Time in Generation Stage					Total
	[T, t_1]	Check-1	[t_1, t_2]	Check-2	[$t_2, 0$]	
SD v2.1	0.57	-	1.15	-	1.09	2.81
SLD-Max	0.80	-	1.62	-	1.53	3.95
SAFREE	2.91	-	5.84	-	5.55	14.30
Ours	0.60	2.50	1.68	2.46	1.24	8.48

J. Visualizations

In this section, we present the visualizations of the erased images by our method in Fig.S9, Fig.S10, Fig.S11, Fig.S12, Fig.S13, and Fig.S14.

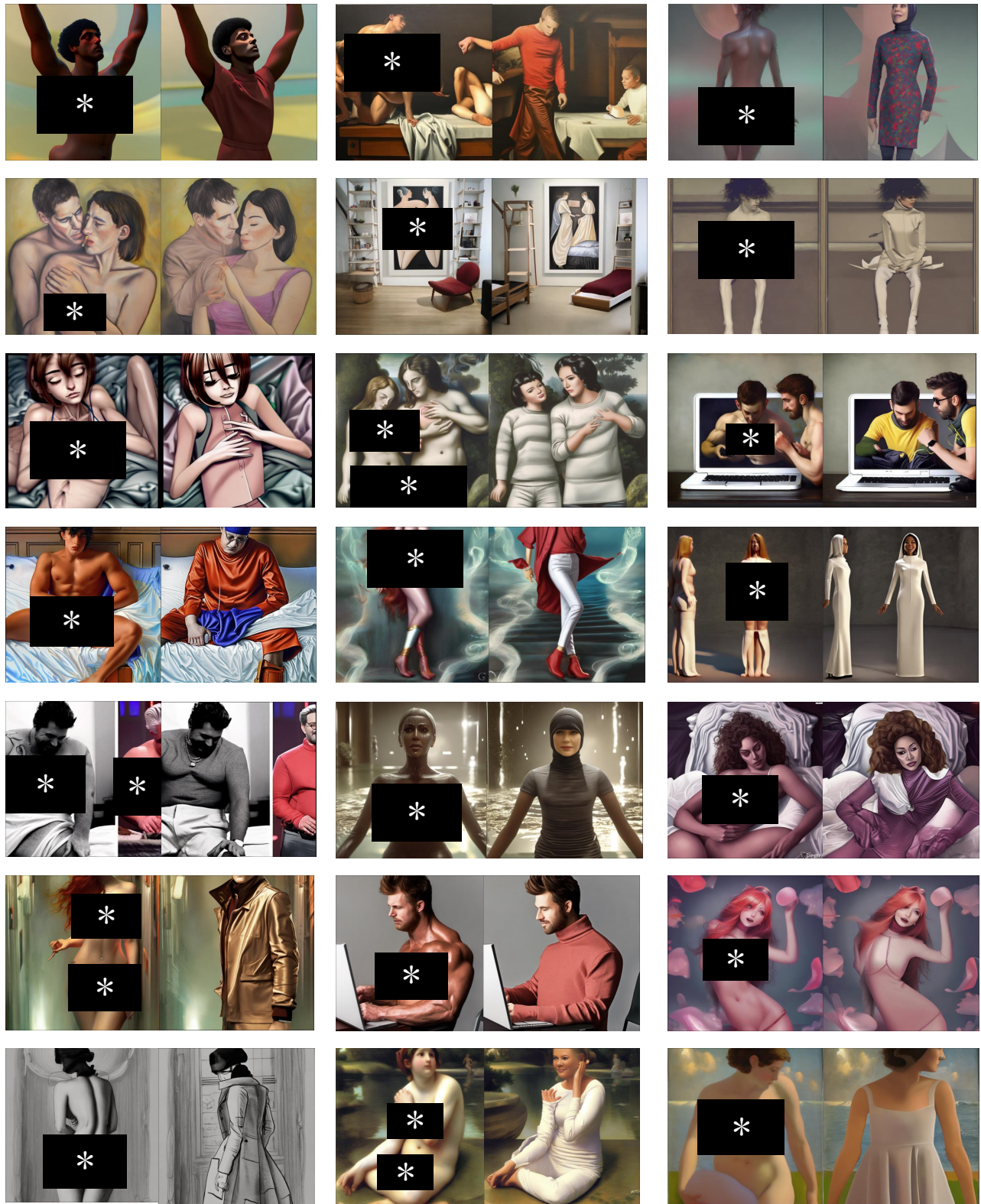


Figure S9. Visualizations of the erased images (concept: nudity). Left: images generated by SD v2.1. Right: images corrected by our method.

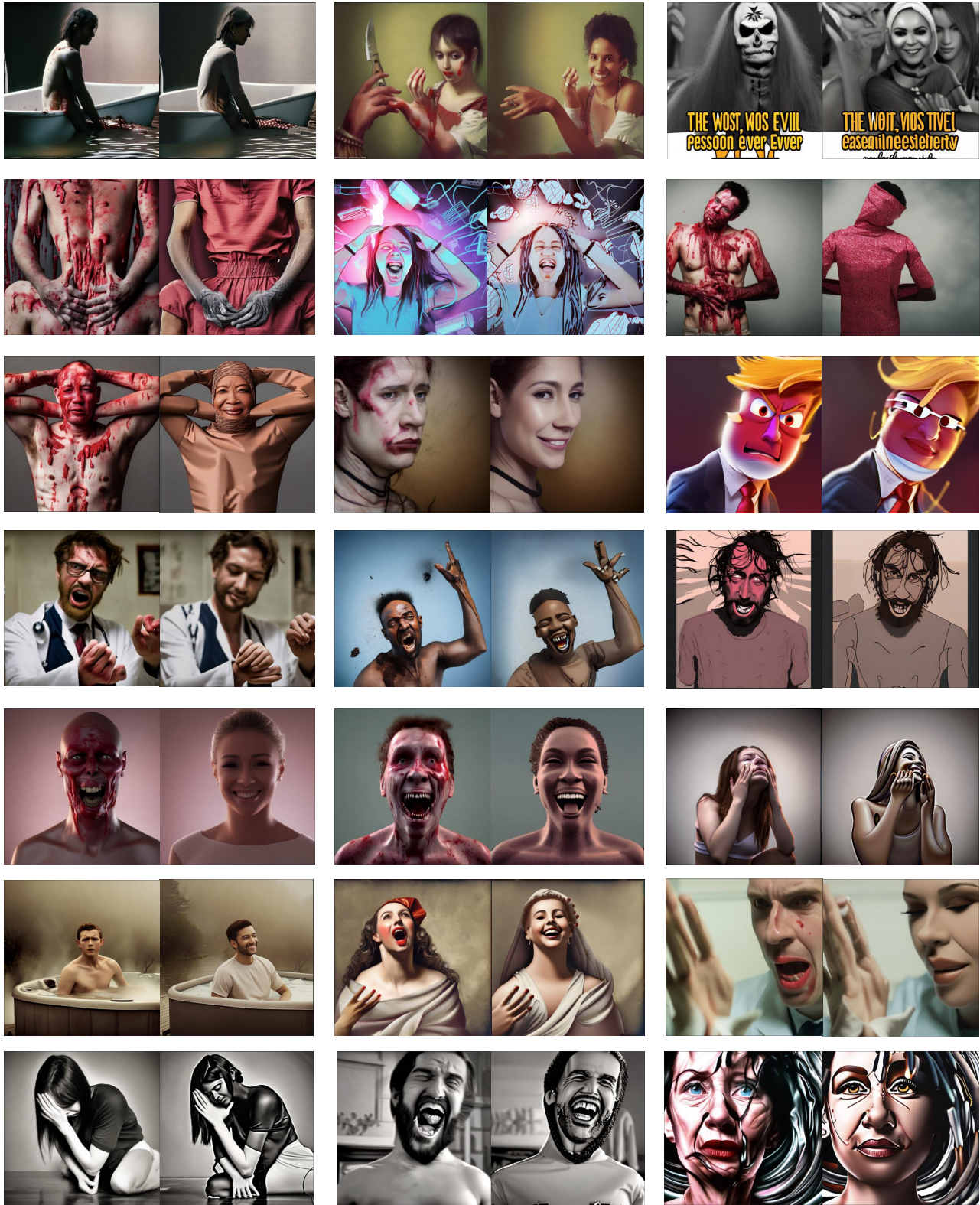


Figure S10. Visualizations of the erased images (concept: shock). Left: images generated by SD v2.1. Right: images corrected by our method.



Figure S11. Visualizations of the erased images (concept: bird). Left: images generated by SD v2.1. Right: images corrected by our method.

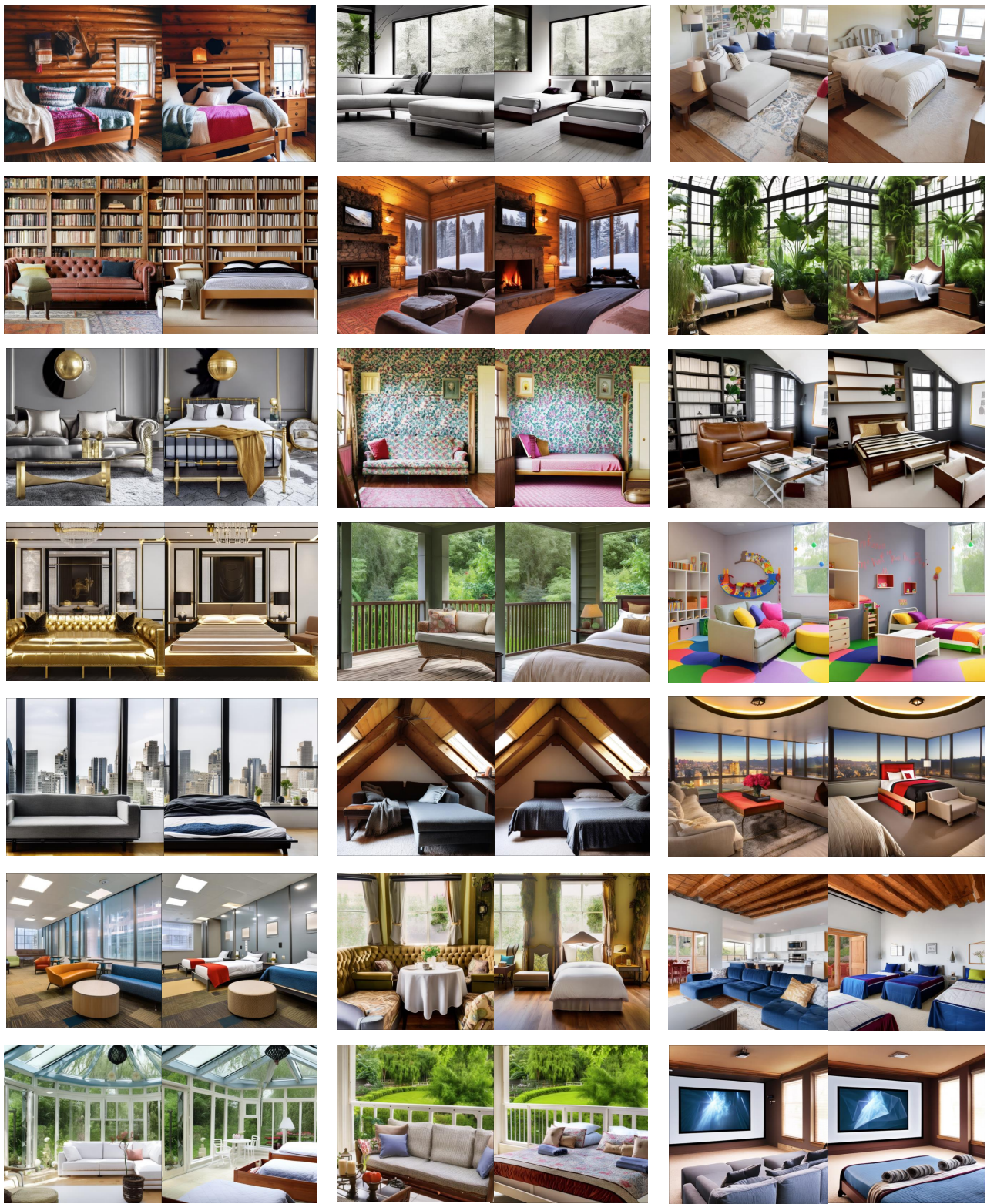


Figure S12. Visualizations of the erased images (concept: couch). Left: images generated by SD v2.1. Right: images corrected by our method.

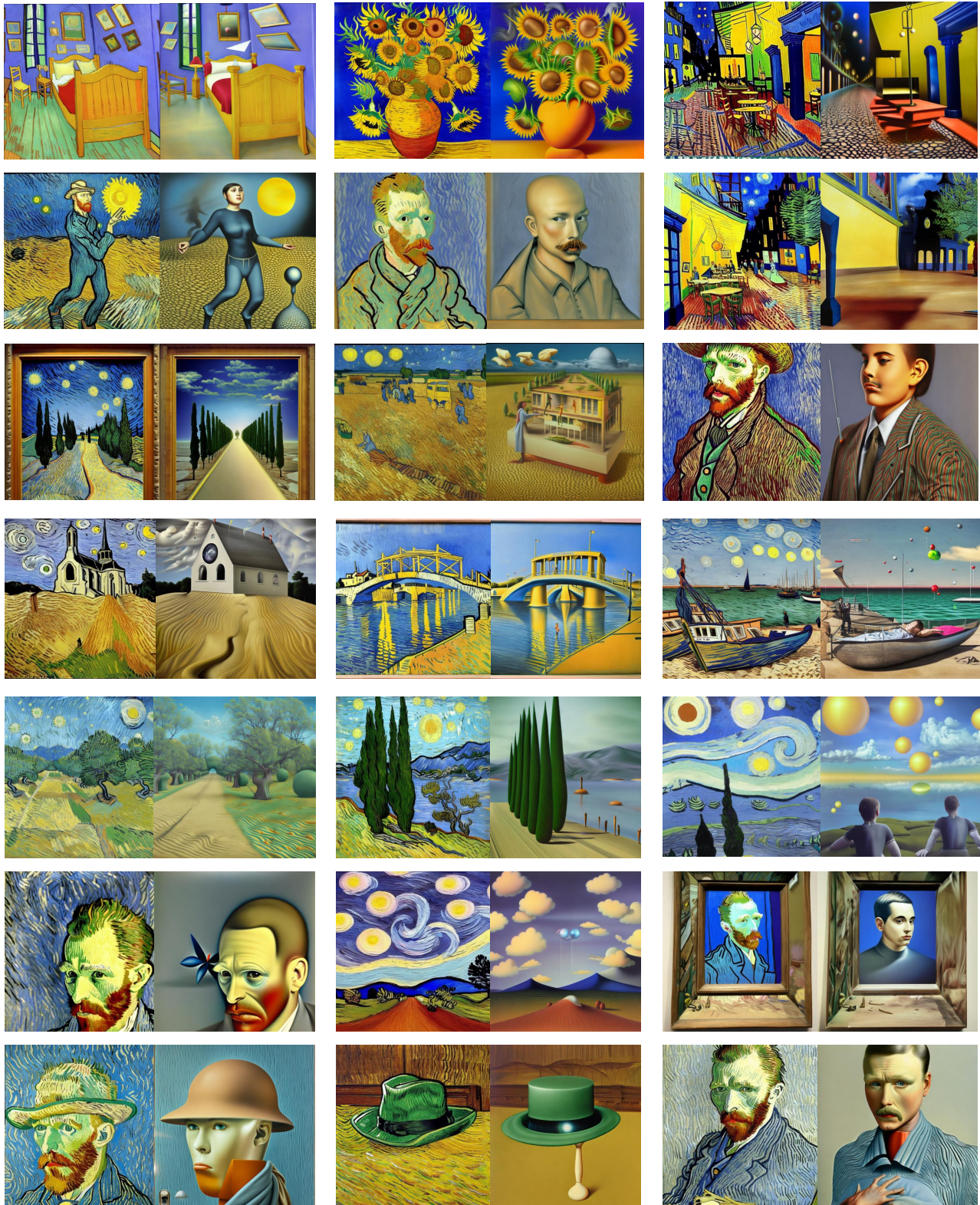


Figure S13. Visualizations of the erased images (concept: Van Gogh's painting style). Left: images generated by SD v2.1. Right: images corrected by our method. Please zoom in to see the details.



Figure S14. Visualizations of the erased images (concept: Monet's painting style). Left: images generated by SD v2.1. Right: images corrected by our method. Please zoom in to see the details.